

Enhanced Electron Transfer for Myoglobin in Surfactant Films on Electrodes

James F. Rusling* and Alaa-Eldin F. Nassar

Contribution from the Department of Chemistry, Box U-60, University of Connecticut, Storrs, Connecticut 06269-3060

Received August 10, 1993*

Abstract: The Fe(III)/Fe(II) redox couple of the heme protein myoglobin (Mb) gave standard electron-transfer rate constants about 1000-fold larger in liquid crystal films of didodecyltrimethyl ammonium bromide (DDAB) on pyrolytic graphite (PG) electrodes than in aqueous solutions. Electron-transfer rates of Mb were also enhanced in films of soluble cationic and anionic surfactants adsorbed on PG. Results suggest a role for strongly adsorbed surfactant at electrode-film interfaces, which may prevent adsorption of macromolecular impurities which can block electron transfer. Mb-DDAB films were prepared by spontaneous insertion of Mb from solution into water-insoluble cast films of DDAB. The resulting films were stable for a month in pH 5.5–7.5 buffers containing 50 mM NaBr. Spectroscopic, thermal, and electrochemical characterizations suggest that the films consist of lamellar liquid crystal DDAB containing preferentially oriented myoglobin with the iron heme in a high spin state. Mb-DDAB films showed good charge-transport rates, which allowed Mb to be used as a redox catalyst. Reductions of the organohalide pollutants trichloroacetic acid and ethylene dibromide were catalyzed by Mb-DDAB films on PG electrodes at voltages 1.0–1.3 V less negative than direct reductions.

Introduction

Reliable methods to improve electron-transfer rates between electrodes and proteins would greatly benefit biosensor and synthetic applications, as well as studies of intrinsic redox properties of proteins.^{1,2} Some proteins containing redox-active prosthetic groups, including myoglobin,³ exchange electrons very slowly with bare electrodes. Considerable research has been directed toward modifying electrodes with promoters¹ and designing polymeric systems² that increase electron-transfer rates between electrodes and prosthetic groups in proteins.

An ongoing interest in our laboratory has been the development of catalytic systems organized by surfactants to reductively dehalogenate organohalide pollutants.⁴ We wished to explore an enzyme or protein immobilized in a surfactant film on an electrode that could catalyze such reactions in the hope of providing low-energy, selective dehalogenation systems. If such a system features surfactant bilayers resembling biomembranes, it might also provide an experimental model for reductive dehalogenation of pollutants in living systems such as mammalian livers^{5a} and anaerobic bacteria.^{5b} Since many proteins are bound onto or within lipid membranes in living cells,⁶ protein-surfactant films could prove to be useful general models.

Myoglobin (Mb) is an oxygen-transport protein in mammalian muscle. It has a molecular weight (MW) of about 17 000 and contains a single electroactive iron heme as a prosthetic group.³ In the Fe(II) form, Mb reduces organohalides.⁷ Also, Mb has been incorporated in bilayer vesicles and multibilayer surfactant

films.⁸ A preferred orientation of Mb was reported in cast films of a double-chain surfactant with an anionic phosphate head group.⁸

We recently reported incorporation of anionic metal pathalocyanines into cast films of didodecyltrimethylammonium bromide (DDAB), and we used these stable films to catalyze reductive dechlorination.⁹ These DDAB films are lamellar liquid crystals at room temperature. This fluid state facilitates good mass and charge transport necessary for catalytic applications.¹⁰

We wished to combine the properties of DDAB films and the reactivity of Mb. We report herein the preparation of stable Mb-DDAB films on pyrolytic graphite (PG) electrodes. Heterogeneous electron-transfer rates on pyrolytic graphite for the Mb Fe(III)/Fe(II) redox couple in these films are enhanced up to 1000-fold over those in aqueous solution. Mb-DDAB films catalyzed electrochemical reduction of ethylene dibromide and trichloroacetic acid with a large decrease in activation energy.

Experimental Section

Materials. Lyophilized myoglobin from horse skeletal muscle (Sigma) was dissolved in buffers of acetate/acetic acid, pH 5.45, or tris-(hydroxymethyl)aminomethane/Tris-HCl, pH 7.5. Buffers were 0.01 M in the conjugate base and contained 50 mM NaBr. Myoglobin solutions were filtered through a YM30 filter (Amicon, 30 000 MW cutoff) to remove higher molecular weight species,^{11,12} which may interfere with electron transfer.^{3,11} Gel permeation chromatography¹² of filtered samples showed Mb with MW 17 100 as the only protein present in this MW range.

Didodecyltrimethylammonium bromide (DDAB, 99%) was from Eastman Kodak, and cetyltrimethylammonium bromide (CTAB) was

* Abstract published in *Advance ACS Abstracts*, November 15, 1993.

(1) (a) Armstrong, F. A.; Hill, H. A. O.; Walton, N. J. *Acc. Chem. Res.* **1988**, *21*, 407–413. (b) Armstrong, F. A. *Bioinorganic Chemistry: Structure and Bonding* 72; Springer-Verlag: Berlin, 1990; pp 137–221.

(2) Heller, A. *Acc. Chem. Res.* **1990**, *23*, 128–134.

(3) King, B. C.; Hawkrigge, F. M.; Hoffman, B. M. *J. Am. Chem. Soc.* **1992**, *114*, 10603–10608 and references therein.

(4) Rusling, J. F. *Acc. Chem. Res.* **1991**, *24*, 75–81.

(5) (a) Pryor, W. A. In *Free Radicals in Biology*; Pryor, W. A., Ed.; Academic: New York, 1976; pp 1–50. (b) Brown, J. F.; Bedard, D. L.; Brennan, M. J.; Carnahan, J. C.; Feng, H.; Wagner, R. F. *Science* **1987**, *236*, 709–712.

(6) Kotyk, A.; Janacek, K.; Koryta, J. *Biophysical Chemistry of Membrane Function*, Wiley: Chichester, U.K., 1988; pp 41–115.

(7) (a) Wade, R. S.; Castro, C. E. *J. Am. Chem. Soc.* **1973**, *95*, 231–234. (b) Bartnicki, E. W.; Belsler, N. O.; Castro, C. E. *Biochemistry* **1978**, *17*, 5582–5586.

(8) (a) Hamachi, I.; Noda, S.; Kunitake, T. *J. Am. Chem. Soc.* **1990**, *112*, 6744–6745. (b) Hamachi, I.; Honda, T.; Noda, S.; Kunitake, T. *Chem. Lett.* **1991**, 1121–1124. (c) Hamachi, I.; Noda, S.; Kunitake, T. *J. Am. Chem. Soc.* **1991**, *113*, 9625–9630.

(9) (a) Rusling, J. F.; Hu, N.; Zhang, H.; Howe, D.; Miaw, C.-L.; Couture, E. In *Electrochemistry in Colloids and Dispersions*; Mackay, R. A., Texter, J., Eds.; VCH Publishers: New York, 1992; pp 303–318. (b) Rusling, J. F.; Ahmadi, M. F.; Hu, N. *Langmuir* **1992**, *8*, 2455–2460. (c) Miaw, C.-L.; Hu, N.; Bobbitt, J. M.; Ma, Z.; Ahmadi, M. F.; Rusling, J. F. *Langmuir* **1993**, *9*, 315–322. (d) Zhang, H.; Rusling, J. F. *Talanta* **1993**, *40*, 741–747.

(10) Rusling, J. F.; Zhang, H. *Langmuir* **1991**, *7*, 1791–1796.

(11) (a) Taniguchi, I.; Watanabe, K.; Tominaga, M.; Hawkrigge, F. M. *J. Electroanal. Chem.* **1992**, *333*, 331–338. (b) Hawkrigge, F. M., private communication.

(12) Walker, J. M., Ed. *Methods in Molecular Biology, Vol. 1, Proteins*; Humana Press: Clifton Heights, NJ, 1984.

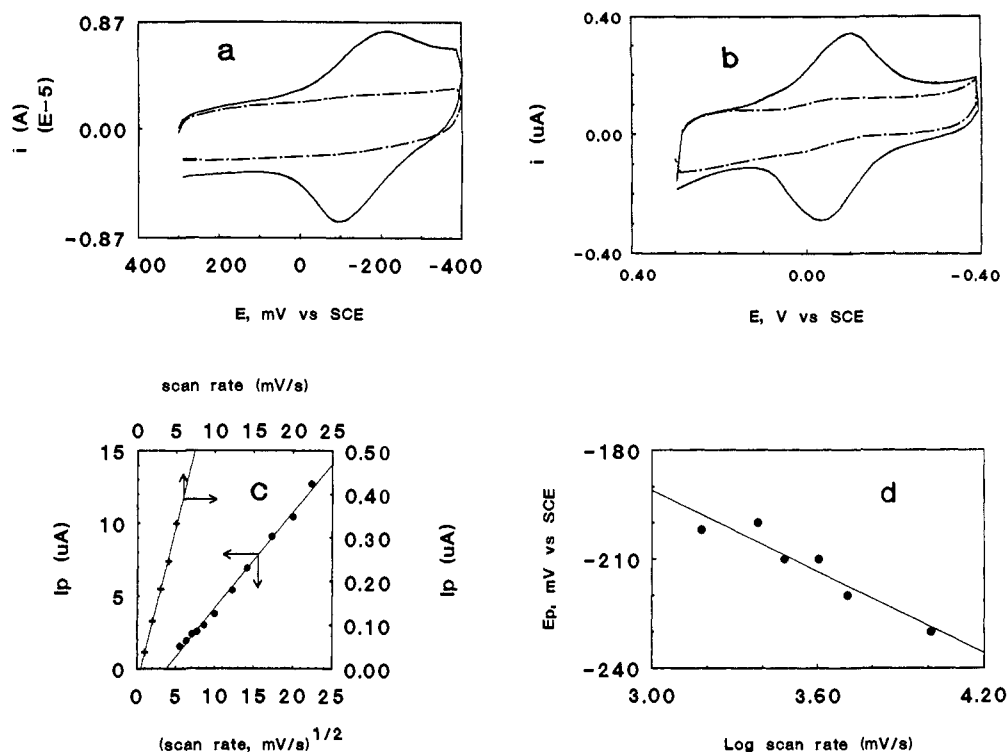


Figure 1. Representative voltammetric results for Mb-DDAB-PG in buffers containing 50 mM NaBr. (a) CVs at 100 mV s⁻¹ in pH 7.5 buffer: dashed line for 0.5 mM Mb on bare PG electrode; solid line for fully loaded Mb-DDAB film, buffer contains no Mb. (b) CVs in pH 5.45 buffer at 5 mV s⁻¹: dashed line for 0.5 mM Mb on bare PG electrode; solid line for fully loaded Mb-DDAB film, buffer contains no Mb. (c) Influence of scan rate on cathodic peak current for Mb-DDAB on PG in pH 7.5 buffer. (d) Influence of scan rate on cathodic peak potential for Mb-DDAB on PG in pH 5.45 buffer.

Fischer Certified (99.8%). Sodium dodecyl sulfate (SDS) was from Aldrich. Water was purified with a Barnstead nanopure system to specific resistance >15 Ω-cm. All other chemicals were reagent grade.

Apparatus and Procedures. Voltammetry. A Bioanalytical Systems BAS-100 and a PARC Model 273 were used for cyclic voltammetry (CV) and normal pulse voltammetry (NPV). The three-electrode cell employed a saturated calomel reference electrode (SCE), a Pt wire counter electrode, and a basal plane pyrolytic graphite (HPG-99, Union Carbide) disk (geometric $A = 0.2 \text{ cm}^2$) working electrode. For the latter, PG cylinders were connected to glass tubes with heat shrinkable tubing and abraded with 600-grit SiC paper on a metallographic polishing wheel prior to coating with surfactant films, as described previously.^{9a,13} Pt disk electrodes were also used for a few experiments.

Surfactant coatings were cast onto electrodes as described previously.^{9,10} Freshly abraded PG discs were coated, typically, with 10 μL of 0.1 M DDAB (1 μmol total, $5 \times 10^{-6} \text{ mol cm}^{-2}$) in chloroform. Film thickness estimated from the amount of DDAB used is ca. 20 μm.¹⁰ Chloroform was evaporated gradually overnight after a small bottle was fit tightly over the electrode to serve as a closed evaporation chamber, followed by a period of standing in air. DDAB-PG electrodes were placed into buffered 0.1–0.5 mM Mb solutions, with potential scanning until steady-state CVs were observed.

When treated with soluble surfactants, PG electrodes were sonicated for 2 min in 0.1 M SDS or CTAB solutions, washed, and then placed into a buffered 0.1 mM Mb solution for 30 min, with intermittent potential scanning until a steady-state CV was observed.

CVs for Mb-surfactant film characterization were done after transfer of the electrode to buffers containing no Mb.

Electrochemical experiments were thermostated at 25 °C. The buffer and sample solutions were purged with purified nitrogen for at least 20 min to remove oxygen prior to the beginning of a series of experiments. Nitrogen atmosphere was maintained over the solutions during the experiments. Removal of oxygen is very important in these systems, since a large catalytic oxygen wave is observed for Mb-DDAB films in unpurged solutions. Ohmic drop of the cells was compensated to >90% for CV and NPV, with typical uncompensated resistance of 20–50 Ω. The actual area of the working electrodes was 0.37 cm², estimated from the slope of the linear scan rate dependence of CV peak current of 1 mM potassium hexacyanoferrate in 1 M KCl ($7.63 \times 10^{-6} \text{ cm}^2 \text{ s}^{-1}$).¹⁴

Structural Characterization. Energy dispersive X-ray analysis (EDX) was done with an Amray 1810 scanning electron microscope (SEM) using a tungsten filament as electron source, as described previously.¹³

DDAB films for SEM/EDX were coated onto PG electrodes and loaded with Mb as for voltammetry.

Differential scanning calorimetry (DSC) was done with a Perkin-Elmer Model DSC-7 calorimeter, with a cell volume of 20 μL under 3 atm to prevent degassing during heating, and calibrated with pure water (0.0 °C) and indium (156.6 °C). Thick DDAB films (5–10 mg) were prepared as above on PG disks and equilibrated with Mb solutions until steady-state CVs were obtained. The films were removed from solution just before DSC and then scraped off the PG into aluminum sample pans, which were then crimped shut. Samples were held at 5 °C for 10 min. Analytical scans at 5 °C min⁻¹ were subsequently initiated. Phase transitions are reported as onset temperatures of peaks in the thermograms.

Absorption spectroscopy was done by using a Perkin-Elmer λ6 UV-vis spectrophotometer. Films were deposited onto quartz slides. These films were soaked in 0.2 mM Mb solutions for several hours. Films were air-dried before spectra were obtained. Matched dichroic sheet polarizers (Melles Griot) were used for linear dichroism.

Reflectance-absorbance infrared spectra (RAIR) and transmission IR spectra were obtained by using a Mattson Galaxy 6020 FT-IR spectrometer with a liquid nitrogen-cooled MCT detector at 4-cm⁻¹ resolution. RAIR spectra were obtained by using a SPECAC variable incident angle accessory with a wire grid polarizer of KRS-5, as described previously.¹⁵ Films were cast onto vapor-deposited aluminum coated onto glass slides. Spectra of the aluminum underlayers were subtracted as background.

Results

Electrochemical Reduction. Myoglobin (Mb) was investigated in pH 5.45 and 7.5 buffers containing 50 mM NaBr. In this pH range at the ionic strengths used, Mb has its native secondary structure.¹⁶ Solutions of lyophilized Sigma Mb used directly or filtered through 30 000 MW cutoff filters gave cyclic voltammograms on PG or platinum electrodes (Figure 1a,b) that were

(13) Hu, N.; Howe, D. J.; Ahmadi, M. F.; Rusling, J. F. *Anal. Chem.* **1992**, *64*, 3180–3186.

(14) Adams, R. N. *Electrochemistry at Solid Electrodes*; Marcel Dekker: New York, 1969.

(15) Suga, K.; Rusling, J. F. *Langmuir*, in press.

(16) (a) Goto, Y.; Fink, A. L. *J. Mol. Biol.* **1990**, *214*, 803–805. (b) Stigter, D.; Alonso, D. O. V.; Dill, K. A. *Proc. Natl. Acad. Sci. U.S.A.* **1991**, *88*, 4176–4180.

Table I. Electrochemical Parameters for Myoglobin at 25 °C

pH	sample/electrode	method	$10^6 D'$, cm ² /s	E° , V/NHE	$10^3 k^\circ$, cm/s	ref
5.5 ^a	Mb-DDAB ^b -PG	CV	0.51 ^d	0.12	6.7 ± 0.7	tw ^g
		NPV	0.57 ^d	0.065	7.1 ± 1.5	tw
7.5 ^a	Mb-DDAB ^b -PG	CV	0.37 ^d	0.05	9.0 ± 0.3	tw
		NPV	0.44 ^d	0.06	7.8 ± 1.5	tw
5.5 ^a	Mb-CTAB-PG ^c	CV	0.8 ^e	-0.02	1.1 ± 0.2	tw
		NPV	0.3 ^e	0.055	5.0 ± 2.0	tw
5.5 ^a	aqueous Mb/CTAB-PG	CV	0.4 ^e	-0.014	0.8 ± 0.4	tw
5.5 ^a	Mb-SDS-PG ^c	CV	0.1 ^e	-0.035	1.1 ± 0.1	tw
		NPV	0.5 ^e	-0.024	3.7 ± 1.4	tw
5.5-7.5 ^a	aqueous/bare PG	CV			ND ^f	tw
7.0	aqueous/bare InSnO ₂	CV	0.5	0.05	0.007	3
7.0	aqueous + CN ⁻ /InSnO ₂	CV	0.5	-0.385	0.7	3
6.5	aqueous/InSnO ₂ + anionic surfactant	CV	0.5	0.06	0.3	11

^a Solutions contained 50 mM NaBr. ^b Films fully loaded with Mb in buffer solutions without Mb. ^c See text for preparation. ^d D_{ct} using measured concentration of Mb and estimated thickness of 20 μm. ^e D_{ct} approximated by using solution Mb concentration. This is an apparent D_{ct} which implicitly assumes a Mb partition coefficient of 1 and reflects the inherent error in this assumption. ^f No peaks detected. ^g This work.

similar to background curves in buffers without Mb. No peaks were found. This is in contrast to the behavior at InSnO₂ cathodes, for which slow electron transfer to aquometmyoglobin [H₂-OMbFe^{III}] to yield MbFe^{II} was reported (Table I).³

When PG electrodes coated with 1 μmol of DDAB were placed into buffered Mb solutions, repetitive CV scanning revealed the growth of a cathodic-anodic peak pair near -0.1 V vs SCE. Steady-state CVs representing films fully loaded with Mb were achieved in ca. 15 min (Figure 1a,b). Similar CVs were obtained after the DDAB-PG electrode was allowed to stand in Mb solution for 30 min.

When fully loaded Mb-DDAB films were removed from Mb solutions and transferred to buffers containing 50 mM NaBr but no Mb, stable CVs were obtained. Typically, storage in buffers for 1 month led to only a 10-20% decrease of cathodic peak height at 100 mV s⁻¹.

The experiments described below were done after transfer of Mb-DDAB electrodes to buffers containing no Mb. Results were similar at pH 5.45 and 7.5. CVs at scan rates above 50 mV s⁻¹ had the typical diffusion-controlled shape (Figure 1a). At scan rates below about 6 mV s⁻¹, a more symmetric peak shape was obtained (Figure 1b). At these very low scan rates, peak current was proportional to scan rate (Figure 1c), as expected for thin-layer electrochemical behavior,^{17,18} in which conversion of all the Mb in the film from Fe(III) to Fe(II) occurs.

Integration under the low scan rate cathodic peaks provided average amounts of Mb in fully loaded 1 μmol DDAB films of 0.078 nmol at pH 5.45 and 0.059 nmol at pH 7.5. Using the estimated film volume,¹⁰ Mb concentrations in these films were 0.45 mM at pH 5.45 and 0.35 mM at pH 7.5.

At scan rates above 50 mV s⁻¹, peak currents for Mb reduction in the films were proportional to the square root of scan rate (ν), as expected for diffusion-kinetic-controlled charge transfer at the electrode-film interface (Figure 1c). Peak potentials shifted negative (Figure 1d) by >40 mV/log ν , also consistent with diffusion-kinetic-controlled charge transfer.^{17,18}

Good agreement of experimental data with the diffusion-kinetic model in these relatively thick films at higher scan rates justifies using this model to estimate formal potentials (E°), charge-transport diffusion coefficients¹⁸ (D_{ct}), and apparent standard heterogeneous rate constants (k°)¹⁹ for Mb in the films. Results show (Table I) that rate constants for Mb-DDAB were much larger than those of bare PG, for which electron transfer was not detected, and about 1000-fold larger than those for aquo-Mb on

InSnO₂. Charge-transport diffusion coefficients were similar to actual diffusion coefficients in solution.

Similar experiments were done with PG electrodes which had been sonicated in SDS or CTAB solutions and then placed in 0.1 mM Mb for 30 min, with CV scanning to monitor achievement of steady state. Stable signals resulted for up to 1 week after transfer of these electrodes to Mb-free buffers. For these systems, estimated k° values were slightly smaller (Table I) than those for PG coated with Mb-DDAB but much larger than those on bare electrodes in solution.

Normal pulse voltammetry was used as a second method to estimate electrochemical parameters. The following model was used for determining kinetic parameters for diffusion-kinetic-controlled charge transfer:^{20a}

$$i(t) = i_d \pi^{1/2} \exp(x^2) \operatorname{erfc}(x)/(1 + \theta) \quad (1)$$

where

$$\theta = \exp[(nF/RT)(E - E^\circ)]; \quad i_d = FADC_{Mb}/(\pi^{1/2} t_p^{1/2}) \quad (2)$$

$$x = \kappa(1 + \theta) \theta^{-\alpha} t_p^{1/2} \quad (3)$$

$$\kappa = k^\circ/D^{1/2} \quad (4)$$

where i_d is the limiting current, C_{Mb} is the concentration of Mb in the film, α is the electrochemical transfer coefficient, t_p is the pulse width, D is the diffusion coefficient of oxidized and reduced forms of Mb, assumed to be equal, and the other terms have the usual electrochemical meanings. Equation 1 was fit to NPV data by nonlinear regression analysis using as parameters E° , i_d , κ , and α . A linear background term was also included in the model^{20b} with the slope and intercept as parameters.

The sigmoid-shaped NPV curves were broader at smaller t_p , as expected from the greater influence of charge-transfer kinetics at times several milliseconds after pulse application (Figure 2). Fits of eq 1 to voltammograms obtained for Mb-surfactant films were excellent.

Studies with noisy theoretical data and standard redox systems showed that for parameters in a range similar to those for the Mb films, $t_p \leq 10$ ms gave the most accurate values of kinetic parameter κ , while experiments at $t_p \geq 40$ ms gave the best estimates of D from limiting currents.²¹ This method yielded the parameters in the NPV rows in Table I, in good agreement with the CV results, especially for Mb-DDAB films.

CV was used to estimate how fast Mb reached the electrode surface through a DDAB film previously untreated with Mb. PG electrodes coated with 1 μmol of DDAB were equilibrated with buffer and then transferred to buffer solutions containing 0.2

(17) Bard, A. J.; Faulkner, L. R. *Electrochemical Methods*; Wiley: New York, 1980.

(18) Murray, R. W. In *Electroanalytical Chemistry*, Vol. 13; Bard, A. J., Ed.; Marcel Dekker: New York, 1984; pp 191-368.

(19) (a) Charge-transport diffusion coefficients (D_{ct}) were obtained from the slope of the peak current vs $\nu^{1/2}$ plots,¹⁸ and k° was estimated from the CV peak separations.^{19b} D_{ct} and k° are subject to errors of up to half an order of magnitude due to uncertainty in film thickness. Errors caused by <2 mV in uncompensated ohmic drop were not significant. (b) Nicholson, R. S. *Anal. Chem.* 1965, 37, 1351-1355.

(20) (a) Go, W. S.; O'Dea, J. J.; Osteryoung, J. J. *Electroanal. Chem.* 1988, 255, 21-44. (b) Rusling, J. F. *CRC Crit. Rev. Anal. Chem.* 1989, 21, 49-81.

(21) This is analogous to the usual approach in CV, where lower scan rate data are used to obtain D and faster scan rate data to obtain k° . A full discussion of the NPV method and its errors will be published elsewhere.

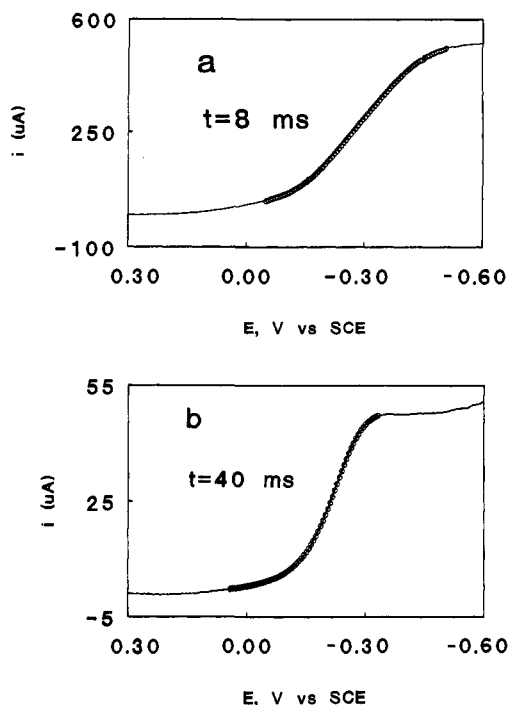


Figure 2. Normal pulse voltammograms for Mb-DDAB on PG in pH 7.5 buffer containing 50 mM NaBr: (a) 8-ms pulse time; (b) 40-ms pulse time. Lines are experimental data, points are best fits to eq 1 by nonlinear regression, found for average parameters $k^{\circ} = 7.8 \times 10^{-3} \text{ cm s}^{-1}$, $D = 4.4 \times 10^{-7} \text{ cm}^2 \text{ s}^{-1}$, $\alpha = 0.3$, and $E^{\circ} = -0.18 \text{ V vs SCE}$.

Table II. Gel-to-Liquid Crystal Phase Transition Temperatures ($^{\circ}\text{C}$)

sample	DSC [ref] ^a	voltammetry [ref]
DDAB bilayer vesicles in water	15 [13]	
DDAB film ^b	11 [13]	
DDAB film ^b + $\text{Fe}(\text{CN})_6^{4-}$	16 [13]	9 [10]
DDAB-Mb film, ^c pH 5.45	12 [tw]	15 [tw]
DDAB-Mb film, ^c pH 7.5	15 [tw]	17 [tw]

^a Five $^{\circ}\text{C}/\text{min}$ scan rate or smaller; tw, this work. ^b Equilibrated with aqueous 0.1 M KBr. ^c Equilibrated with buffer solutions containing 50 mM NaBr.

mM Mb. CVs at 2 V s^{-1} were run periodically to find the time when the Mb peak could be detected. For several electrodes at both pH values, a cathodic peak about 20% of the steady-state peak current was observed within 10–25 s. Thus, the average breakthrough time of the first Mb molecules can be estimated as $<10 \text{ s}$. The root-mean-square displacement Δ^2 is related to the diffusion coefficient by¹⁷

$$\Delta^2 = 2Dt$$

This equation was used to estimate the time t required to pass through a film for a molecule with D_{ct} as estimated for Mb-DDAB. For $D = 4 \times 10^{-7} \text{ cm}^2 \text{ s}^{-1}$, the estimated breakthrough time is 5 s for a 20- μm film.

Phase Transitions. DDAB films undergo transitions from the liquid crystal to the solid-like gel phase below room temperature. This transition is characteristic of surfactant bilayers.^{6,8–10,13} By using differential scanning calorimetry, phase transitions were found for Mb-DDAB films at similar temperatures (T_c) as for other DDAB films and for bilayer vesicles of DDAB (Table II).

If electroactive species are present in cast surfactant films, then the gel-to-liquid crystal phase transition is also reflected in plots of peak or limiting current vs temperature (Figure 3). Breaks in such plots for Mb-DDAB films were generally found at temperatures similar to the T_c values found by DSC^{9,13} (Table II).

Reflectance-Absorbance FT-IR (RAIR). The shapes of the amide I and amide II infrared absorbance bands of proteins provide detailed information on the secondary structure of the polypeptide

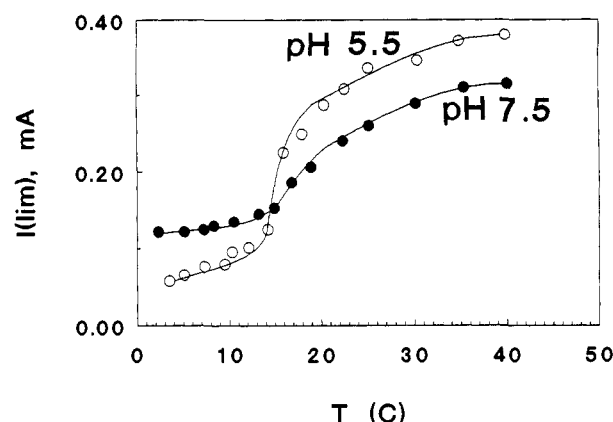


Figure 3. Influence of temperature on NPV limiting current ($t_p = 10 \text{ ms}$) for Mb-DDAB on PG.

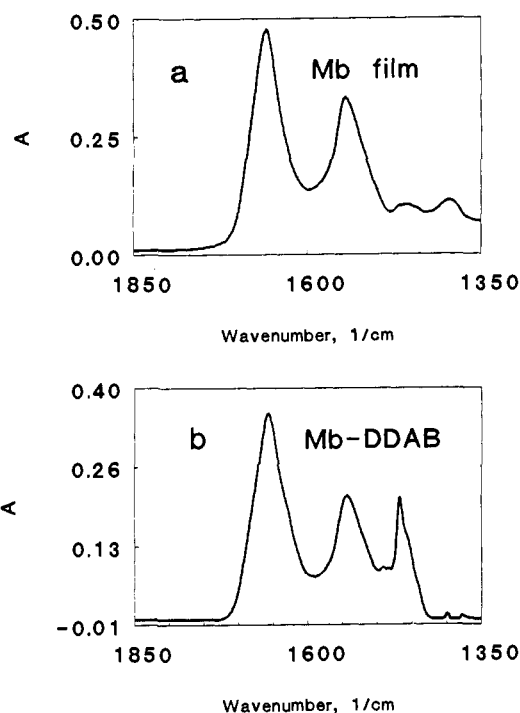


Figure 4. RAIR spectra (60°) for (a) Mb film cast from pH 7.5 buffer; (b) Mb-DDAB film loaded in a pH 7.5 buffer. (Films cast onto aluminum slides.)

chain.^{22,23} These bands are observed in the $1500\text{--}1700\text{-cm}^{-1}$ region in the RAIR spectrum of a film prepared from myoglobin in pH 7.5 buffer (Figure 4a). This spectrum is similar to that of Mb dissolved in pH 7.5 buffer. The amide I and II bands in the RAIR spectrum of Mb-DDAB have shapes similar to that of the film of Mb alone (Figure 4b). The additional band for Mb-DDAB at 1462 cm^{-1} is the CH_2 bending mode of the DDAB hydrocarbon tails.¹⁵

Similarities of spectra in Figures 4a and 4b suggest that Mb retains the essential features of its native structure in the DDAB films.^{24,25} Similar results were obtained at pH 5.45. Purposely denatured samples of Mb showed completely different spectral characteristics in amide I and II regions.

Orientations of the hydrocarbon tails of DDAB in the films were estimated from RAIR data by a previously described method.¹⁵ Briefly, a standard reference peak representing a transition dipole moment normal to the film plane was first

(22) Kauppinen, J. K.; Moffatt, D. J.; Mantsch, H. H.; Cameron, D. G. *Appl. Spectrosc.* **1981**, *35*, 271–276.

(23) Rusling, J. F.; Kumosinski, T. F. *Intell. Instrum. Comput.* **1992**, *10* (July/Aug) 139–145.

(24) Small differences in these spectra are currently under study by deconvolution/regression analysis.²³

(25) Song, Y. P.; Petty, M. C.; Yarwood, J.; Yeast, W. J.; Tsibouklis, J.; Mukherjee, S. *Langmuir* **1992**, *8*, 257–261.

Table III. Tilt Angles of Hydrocarbon Chains in DDAB Films from RAIR^a

film	cos ² α	cos ² β	cos ² γ	γ (tilt angle)
DDAB ^b	0.067	0.051	0.882	20 ± 1
clay-DDAB ^{b,c}	0.188	0.183	0.742	28 ± 2
Mb-DDAB, pH 5.5	0.149	0.132	0.719	34 ± 4
Mb-DDAB, pH 7.5	0.118	0.117	0.765	29 ± 2

^a Angles are averages for five different films; cos² α from 2853-cm⁻¹ band, cos² β from 2927-cm⁻¹ band. ^b From ref 15. ^c Composite film prepared and stored 1 month at ambient conditions.

Table IV. Positions of Mb Heme Soret Band with Order Parameters from Linear Dichroism

sample	buffer	λ _{max} , nm		
		soln	film	S ^a
Mb	acetate + 50 mM NaBr, pH 5.5	409	410	0.05 ± 0.01
Mb-DDAB	acetate + 50 mM NaBr, pH 5.5		413	0.13 ± 0.03
Mb ^b	acetate + 50 mM NaBr, pH 5.5 (denatured Mb) ^b	400		
Mb ^b	pH 5.5 (denatured Mb) ^b in DDAB film		405	
Mb	Tris + 50 mM NaBr, pH 7.5	409	414	0.07 ± 0.02
Mb-DDAB	Tris + 50 mM NaBr, pH 7.5		415	0.17 ± 0.03
Mb ^b	Tris + 50 mM NaBr, pH 7.5 (denatured Mb) ^b	400		

^a Order parameter²⁶ from linear dichroism of films: $S = \Delta A / 3A$ (see text); average of 4–6 films for each. Differences in λ_{max} at different polarizations were negligible. ^b Denatured with urea.^{27c}

identified as the 912-cm⁻¹ C–N peak (μ₀) of films prepared from cetyltrimethylammonium bromide (CTAB). An external reference is required because no DDAB transition dipoles are normal to the film plane. Glancing angle RAIR spectral absorbances (A_{RA}) of films and absorbances of KBr pellets (A_{KBr}) containing components of Mb-DDAB films (μ_i) and those of the reference CTAB (μ₀) were measured under the same conditions. We estimated A_{KBr}(μ_i)/A_{KBr}(μ₀) and A_{RA}(μ_i)/A_{RA}(μ₀) for the CH₂ stretching modes in the sample film and the 912-cm⁻¹ reference band of CTAB. Knowing the weights of surfactants in sample (w_{i,f}) and reference films (w_{0,f}) and in the KBr pellets (w_{i,p} and w_{0,p}), the average orientation angle of the transition dipole moment to the film normal (θ_{i^{av}}) was estimated from:¹⁵

$$\cos^2 \theta_{i^{av}} = \frac{[A_{RA}(\mu_i)/w_{i,f}]/[A_{RA}(\mu_0)/w_{0,f}]}{[A_{KBr}(\mu_i)/w_{i,p}]/[A_{KBr}(\mu_0)/w_{0,p}]} \quad (5)$$

Transition dipole moments for symmetric (ν_s) and antisymmetric (ν_a) stretching modes of CH₂ are normal to the long axis of an *all-trans* methylene chain. The angles to the normal to the plane of the film, α (ν_s, CH₂) and β (ν_a, CH₂), are found from eq 5. The hydrocarbon chain tilt angle (γ) is obtained from:

$$\cos^2 \alpha + \cos^2 \beta + \cos^2 \gamma = 1 \quad (6)$$

Results show (Table III) that hydrocarbon tails in Mb-DDAB and DDAB films are tilted to the normal. Tilt angles in Mb-DDAB are somewhat larger than in pure DDAB films and are closer to values found for an aged clay-DDAB bilayer composite film.

Electronic Spectra and Linear Dichroism. Soret bands of Mb-DDAB films were similar to those of Mb solutions, consistent with native Mb. Solution spectra in water or buffers gave this heme band at 409 nm (Table IV). Mb purposely denatured with urea gave a band at about 400 nm in buffer solutions and at 405 nm in a DDAB film. Films cast from Mb alone gave heme bands at 410 nm at pH 5.5 and at 414 nm at pH 7.5. Values of λ_{max} in the Mb-DDAB film were shifted a few nanometers toward the red (Table IV).

Spectra of films obtained with plane-polarized light showed that the Soret bands had different intensities for parallel and perpendicular polarizations (Figure 5). These linear dichroic differences were larger for Mb-DDAB than for films cast from

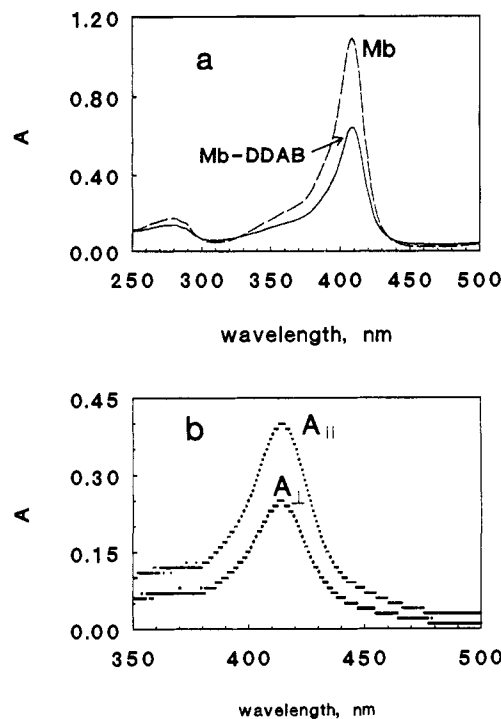


Figure 5. UV-Vis spectra. (a) Unpolarized Mb and Mb-DDAB films on quartz prepared by using pH 5.5 buffers containing 50 mM NaBr. (b) Influence of polarized light for Mb-DDAB films on quartz prepared by using pH 7.5 buffers containing 50 mM NaBr.

Mb alone. An approximate theory²⁶ was used to compute an average order parameter S :

$$S = (1 - 3 \cos^2 \varphi) / 2 \quad (7)$$

from

$$\Delta A / A = 3S \quad (8)$$

where $\Delta A = A_{\parallel} - A_{\perp}$, the difference between the peak absorbances with parallel and perpendicularly polarized light, A is the absorbance of a randomly oriented sample taken²⁶ as $A = (A_{\parallel} + 2A_{\perp}) / 3$, and φ is the angle between the transition moment for the absorption and the normal to the film plane. Order parameters were significantly larger for Mb-DDAB films than for the corresponding Mb films prepared at the same pH values (Table IV). Results suggest a preferred average orientation for the heme group,²⁷ and consequently for Mb, in the DDAB films.

Elemental Analysis. Energy dispersive X-ray analysis was done on films prepared on PG electrodes. One set of films was made 2.5 times thicker than the ca. 20-μm films used for voltammetry so that only the film would be sampled by the source with sampling depth 1–2 μm. Bromine and carbon were the only elements found; iron was not detectable. Average Br/C ratios in buffer-treated DDAB films were more than 3 times larger than those for Mb-DDAB films (Table V). Similar results were obtained for films nominally 25-fold thinner (ca. 2 μm), in which a major fraction of the film was sampled.

Electrochemical Catalysis of Organohalide Reductions. A specific aim of this work was to develop a Mb-DDAB coating capable of reducing organohalides. Reactions of the Fe(II) form of Mb-DDAB with trichloroacetic acid and ethylene dibromide were surveyed by voltammetry. When a Mb-DDAB-PG electrode was placed into a pH 5.5 buffer containing trichloroacetic

(26) (a) Breton, J.; Michel-Villaz, M.; Paillotin, G. *Biochim. Biophys. Acta* 1973, 314, 42–56. (b) The negative of S in eq 8 is also used as an order parameter.^{27b}

(27) (a) Average values of φ for Mb-DDAB films were 62 ± 2° at pH 7.5 and 61 ± 2° at pH 5.5, but these values are not corrected for optical errors, which could lead to bias on the order of 10%.^{27b} Detailed experiments employing appropriate corrections are in progress. (b) Norden, B.; Lindblom, G.; Jonas, I. *J. Phys. Chem.* 1977, 81, 2086–2093. (c) Herskovits, T. T.; Jailet, H.; Gadegebku, B. *J. Biol. Chem.* 1970, 245, 4544–4550.

Table V. Elemental Analysis of Films on PG by EDX^a

film	atom % ^b		
	C	Br	Br/C
dry DDAB	67	33	0.49
DDAB, pH 7.5 ^c	71	29	0.41
Mb-DDAB, pH 5.5 ^c	88	12	0.14
Mb-DDAB, pH 7.5 ^c	94	6	0.06

^a Average values from five spots analyses (1–2- μm diameter) on each of three electrodes. Relative standard deviation about $\pm 10\%$. ^b Nominal values computed for C and Br only from counts per second peak areas and relevant sensitivity factors. ^c Films prepared on PG and soaked overnight in buffer with or without 0.5 mM Mb.

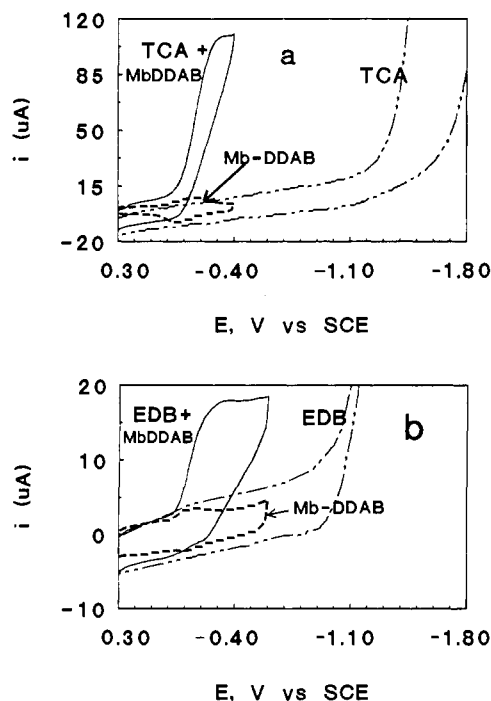


Figure 6. Cyclic voltammograms at 100 mV s^{-1} in pH 5.45 buffers containing 50 mM NaBr. (a) Mb-DDAB-PG electrode without and with 5 mM trichloroacetic acid present; TCA curve at DDAB-PG electrode with 5 mM trichloroacetic acid added. (b) Mb-DDAB-PG electrode without and with 10 mM ethylene dibromide added; EDB curve at DDAB-PG electrode with 10 mM ethylene dibromide added.

acid or ethylene dibromide, an increase in the Mb Fe(III)/Fe(II) reduction peak was observed (Figure 6). This was accompanied by disappearance of the MbFe^{II} oxidation peak, indicating its reaction with the organohalides. The peak reduction current for Mb was linearly proportional to concentration of the organohalides. These results are characteristic^{17,18} of catalytic reduction of the organohalides by Mb in the film. The difference between the half-peak potentials of direct reduction and catalytic reduction of the organohalides was about 1.3 V for trichloroacetic acid and 1.0 V for ethylene dibromide.

Discussion

Structure of Mb-DDAB Films. Gel-to-liquid crystal transition temperature (T_c , Table II) from DSC are similar to those from the temperature dependence of voltammetric current. T_c values for Mb-DDAB films are also similar to those for DDAB bilayer vesicles, suggesting that DDAB in the films is arranged in multiple bilayer structures similar to those proposed for DDAB films containing various counterions.^{9,10,13} This lamellar state contains considerable water between the bilayers.^{6,13}

Significantly larger currents for MbFe^{III} reduction at $T > T_c$, as well as the shapes of i_{lim} vs T curves (Figure 3), can be attributed to faster charge transport in the more fluid liquid crystal phase of the films. Similar results were found for electroactive anions such as ferrocyanide¹⁰ or metal phthalocyanine tetrasulfonate^{9,13}

in DDAB films. A series of such ions gave charge-transport diffusion coefficients^{9,10} (D_{ct}) in the range $0.6\text{--}1 \times 10^{-6} \text{ cm}^2 \text{ s}^{-1}$ in DDAB films, only slightly larger than values for Mb-DDAB (Table I). In addition, values for Mb in DDAB films are similar to the diffusion coefficients of Mb in aqueous solutions. Values of D_{ct} for Mb-DDAB predict breakthrough times of 5 s for a mean free path of 20 μm , consistent with the estimate of <10 s for Mb passing through DDAB films to electrodes. These results suggest physical diffusion of Mb within the films.

Infrared and visible spectra establish that Mb incorporated into the films has a secondary structure close to that of its native state in solutions and Mb films without surfactant. Estimates of tilt angles of the hydrocarbon chains of DDAB (Table III) are somewhat larger than those of pure DDAB films but similar to those of clay-DDAB composites. These tilt angles are similar to those of biological membranes and liposomes.⁶ Results support the multibilayer DDAB structure. RAIIR spectra suggest, however, that Mb-DDAB films may have subtle structural differences from pure DDAB films.²⁴

The Fe(III) in Mb is complexed by the four-coordinate planar porphyrin ring, by a histidine from the protein at one axial site, and by another labile axial ligand that determines the spin state.³ The λ_{max} values of 413–415 nm for Mb-DDAB are closer to the 411 nm reported for the crystalline high-spin aquoMb²⁸ than to the low-spin values of 426 and 422 nm for CNMb and azideMb crystals, respectively. Positions of Soret bands in Mb-DDAB films are indicative of native Mb with the heme in a high spin state. Electron spin resonance (ESR) spectra also indicate that Mb in DDAB films is predominantly high spin.²⁹ This state features a weak axial ligand on the Fe(III).

Linear dichroism results suggest that Mb has a preferred orientation in DDAB films. The order parameters (Table IV) are of similar magnitude to those for the Mg porphyrin chlorophyll *a* in ordered lamellar films of chloroplasts cast from aqueous solutions ($S = 0.17$).²⁶ Since the Fe(III) heme responsible for the Soret absorbance has its transition moment in the plane of the porphyrin ring,²⁸ the φ value obtained²⁷ from order parameter S (eq 7) represents an estimate of the angle between the normal to the film plane and the plane of the Fe(III) heme.

In previous studies on Mb in multibilayer films of a double-chain phosphate surfactant, Kunitake et al. proposed that Mb is intercalated and oriented between surfactant bilayers by interactions with the anionic phosphate groups.^{8a,b} In contrast, we feel that there is not yet sufficient experimental evidence to pin down the exact location of Mb in static Mb-DDAB films. Kunitake et al. also reported partial denaturation of Mb in films of a cationic surfactant different from DDAB. We find no evidence for denaturation of Mb in DDAB films by IR, visible, or ESR²⁹ spectroscopy.

Buffer solutions alone did not replace large amounts of Br⁻ from DDAB films in the absence of protein (Table V). However, a large decrease in Br⁻ content was found for films equilibrated with Mb in the same buffers. This cannot be explained entirely by interactions of anionic amino acid residues of Mb with DDAB head groups. Calculations based on the amounts of DDAB and Mb in fully loaded films indicate that less than 5% of the head-group charge can be compensated by Mb carboxyl groups. One possibility is that Mb may bring bound anions³⁰ from the solution along with it into the film and these may be shared with or donated to the head groups.

The retention and stability of Mb in surfactant films, about 1 month for Mb-DDAB in buffers containing 50 mM NaBr, is rather remarkable. In comparison, ferrocyanide¹⁰ and cobalt(III) corrinhexacarboxylate^{9c} ions are retained only for several hours in solutions containing 0.1 M KBr. Metal phthalocya-

(28) Eaton, W. A.; Hochstrasser, R. M. *J. Chem. Phys.* 1968, 49, 985–995.

(29) Rusling, J. F.; Nassar, A. F.; Kumosinski, T. F., ACS Symposium Series, in preparation.

(30) Antonini, E.; Rossi-Bernardi, L.; Chinacone, E., Eds. *Methods in Enzymology*, Vol. 76, Academic: New York, 1981; pp 552–559.

ninetetrasulfonates are retained for up to 2 weeks in 0.1 M KBr, a property probably related to dimerization of phthalocyanine-tetrasulfonates in the films.¹³

An ion-exchange driving force for entry of the above metal complex multianions into DDAB films is apparent. On the other hand, Mb has a 1+ charge at pH 7.5 and a 6+ charge at pH 5.5.³¹ However, Mb has 20 carboxylate residues³² which might interact with cationic head groups, replacing charge-pair interactions of amino acid residues known to occur on the Mb surface.³³ There also remains the possibility that Mb interacts with hydrophobic regions of bilayers. We are exploring these factors by detailed spectroscopic and molecular dynamics studies.²⁹

Electron-Transfer Reactions. The rate of Mb Fe(III)/Fe(II) electron transfer at PG is about 1000 times faster in DDAB films than in solutions at InSnO₂ electrodes (Table I). Electron transfer between PG and Mb in solution could not be detected. Possible reasons for faster electron transfer in the DDAB films include (i) strong adsorption of surfactant onto the electrode that inhibits adsorption of macromolecular impurities from solution^{1,3,11} which can block electron transfer and (ii) arrangement of Mb in the film in a favorable orientation for exchanging electrons with the electrode. Although faster electron transfer has been found in solution with the low-spin cyano heme complex of Mb (Table I) than with high-spin Mb,³ there is clear evidence that Mb in DDAB films is high spin. Also, the standard potential at pH 7.5 in DDAB films is very close to that of Mb in pH 7 solutions. Thus, water may be Fe(III)'s axial ligand in Mb-DDAB films.

PG electrodes treated with soluble surfactants SDS and CTAB gave faster Mb electron transfer than in solution but slightly slower than in DDAB films. D' is an apparent value, in these cases estimated without knowledge of the actual Mb concentration in the films.

The stability of Mb-CTAB and Mb-SDS films is good. This suggests strong interactions of Mb with these two adsorbed surfactants of different head-group sign. Enhanced electron transfer was also found for cytochrome *c* when Pt electrodes were treated with the surfactants lauric acid and laurylamine.³⁴

The similar kinetic trends found with different types of surfactants suggest that surfactant adsorption on the electrode must play a role in the rate enhancement. However, this conclusion does not rule out an influence for Mb orientation. Linear dichroism suggests orientation of Mb in the DDAB films. Orientation in films of SDS and CTAB may also occur. However, the exact influence of Mb orientation on electron-transfer kinetics remains uncertain.

The site of Mb residence at the time of electron transfer with PG may be a key dynamic feature of the system. Let us assume that the electrode is covered by strongly adsorbed surfactant, as it must be before Mb is introduced.³⁵ If Mb resides on the outer

surface of a bilayer of DDAB at the PG-film interface, it would be at least 30 Å (the width of a tilted DDAB bilayer) away from the electrode. Based on the influence of distance on electron-transfer kinetics,³⁶ transfer of an electron across this distance would be slow. This argument, as well as Mb breakthrough times consistent with predictions from D_{ci} , leads to the suspicion that Mb might be able to pass through the fluid DDAB bilayers in some way during the dynamic voltammetric experiments. Although passage through intact bilayers might be slow, one speculation is that Mb might pass through transient defects in individual bilayers. Such defects occur in biomembranes and are accentuated by relatively small electric fields.⁶

As shown by the catalytic reduction of organohalides, Mb can be made to act as a redox protein in DDAB films on electrodes. This was previously demonstrated in vesicle suspensions, in which Mb reduced by NADH was used to catalytically reduce dioxygen and naphthoquinone sulfonate.^{8c} In the present work, Fe^{II}Mb formed in the Mb-DDAB film by injecting electrons from the electrode reduces trichloroacetic acid and ethylene dibromide (Figure 6). The large 1.0–1.3-V decrease in negative electrode potential for these reactions suggests that Mb-DDAB films might be useful for practical applications in destroying or sensing pollutants. Catalysis with Mb-DDAB requires less activation energy to reduce these organohalides than alternative metal macrocyclic catalysts. Vitamin B₁₂, for example, requires electrode potentials about 0.5 V more negative than those required by Mb-DDAB to catalyze these same reactions.³⁷

Conclusions

Myoglobin forms stable films with water-insoluble, lamellar liquid crystal DDAB by spontaneous insertion from aqueous solutions. Mb also forms films with SDS and CTAB adsorbed on PG electrodes. Electron-transfer rates enhanced up to 1000-fold for the Mb Fe(III)/Fe(II) redox couple appear to be related to adsorbed surfactant at the electrode-film interface, which can inhibit adsorption of macromolecular impurities on the electrode. Mb is oriented in DDAB films. Mb-DDAB films on electrodes catalyzed reduction of two organohalide pollutants with a large decrease in electrode potential.

Acknowledgment. This work was supported by U.S. PHS Grant No. ES03154 from NIH, awarded by the National Institute of Environmental Health Sciences. The authors thank Thomas F. Kumosinski of the U.S. Department of Agriculture for helpful discussions.

(35) (a) Head-down bilayers of DDAB and CTAB at electrode-film interfaces have been inferred^{35b} from surface-enhanced Raman spectroscopy of cast films on silver. There is evidence that head-down orientation of these surfactants and SDS may occur over a wide potential range when adsorption occurs from a relatively concentrated solution.^{35c} (b) Suga, K.; Bradley, M.; Rusling, J. F. *Langmuir*, in press. (c) Rusling, J. F. In *Electroanalytical Chemistry*, Vol. 18; Bard, A. J., Ed.; Marcel Dekker: New York, 1994; pp 1–88.

(36) (a) Closs, G. L.; Miller, J. R. *Science* 1988, 240, 440. (b) Mayo, S. L.; Ellis, W. R.; Crutchley, R. J.; Gray, H. B. *Science* 1986, 233, 948.

(37) (a) Connors, T. F.; Arena, J. V.; Rusling, J. F. *J. Phys. Chem.* 1988, 92, 2810–2816. (b) Rusling, J. F.; Miaw, C.-L.; Couture, E. C. *Inorg. Chem.* 1990, 29, 2025–2027.

(31) (a) Shire, S. J.; Hanania, G. I. H.; Gurd, F. R. N. *Biochemistry* 1974, 13, 2967–2980. (b) Friend, S. H.; Gurd, F. R. N. *Biochemistry* 1979, 18, 4612–4619.

(32) Antonini, E.; Brunori, M. *Hemoglobin and Myoglobin in their Reactions with Ligands*; North Holland: Amsterdam, 1971.

(33) Friend, S. H.; Gurd, F. R. N. *Biochemistry* 1979, 18, 4620–4630.

(34) Guerrieri, A.; Cataldi, T. R. J.; Hill, H. A. O. *J. Electroanal. Chem.* 1991, 297, 541–547.